# Efficient dynamic resource management for OFDMA-MIMO wireless transmission

ALBERT MRÁZ, TAMÁS ZÁMBÓ, SÁNDOR IMRE

*Budapest University of Technology and Economics, Department of Telecommunications*
*{mraz, imre}@hit.bme.hu*

*Keywords: OFDMA, MIMO, carrier allocation, scheduling, antenna selection*

**Efficient radio resource allocation algorithm is proposed for multiuser MIMO-OFDMA environment providing proportional fairness. Familiar MIMO radio channel model is extended for OFDMA transmission, to exploit multiuser diversity. Antenna selection is realized in order to maximize the overall data rate based on MIMO channel estimation. Adaptive M-QAM modulation is performed on selected antennas on each subcarrier, taking into account singular value decomposition based channel gain values arisen from the analytical calculation of MIMO channel capacity. Transmit power control is included over subcarriers and transmit antennas.**

## 1. Introduction

The 4G mobile telecommunications systems are inspired to treat raising user demands in terms of data rate in 3G standards. The key advantages of 4G systems lie on the background of the physical layer access; OFDM (Orthogonal Frequency Division Multiplexing) modulation means an efficient and robust technique which is capable to combat fast variations and the frequency selectivity of the radio channel. OFDMA (Orthogonal Frequency Division Multiple Access) provides further advance in terms of spectral efficiency through location dependent multiuser-diversity [1], and represents the most efficient multiple access technique based on OFDM modulation [2].

Applying MIMO (Multiple-Input and Multiple-Output) antenna solution within a radio communication link is – in principle by the fruition of certain channel properties – able to multiple the attainable data rate by a factor which is determined by the number of transmit and receiver antennas. Hence, the combination of OFDMA and the MIMO antenna solution could step forward to be the key element of 4G radio telecommunication systems physical access, as it is mentioned in WiMAX [3] and LTE [4].

In the current work we are dealing with adaptive downlink radio resource allocation in MIMO-OFDMA systems. The subcarriers defined by the OFDMA scheme are shared among multiple users within the system, aiming maximal system channel capacity along such contradicting requirements like user fairness and maximal available transmit power, while the potential of multiple antennas was also taken into account. The optimization possibilities for a typical MIMO-OFDMA scheduling algorithm are the subcarrier allocation, the adaptive transmit power control over subcarriers, antenna selection at the transmitter side, transmit power control for antennas on selected subcarriers [5,6]. The optimization task is similar to OFDMA physical resource management, except the appearance of additional dimensions in the optimization task, generated by the transmitter and receiver antennas. The multiple antenna transmission enhances the efficiency of the communication, and provides further exploitable optimization gain in the overall transmission rate with the possibility of antenna selection. However, the appearance of a new dimension, the MIMO-OFDMA optimization task becomes to a more difficult problem than 'simple' OFDMA optimization, which is an *NP-hard* computational problem in itself [7].

A suboptimal transmit power control (scheduler) algorithm addressing the described problem, published in [6] was taken as a basis. As the new technical content of this paper, we came up with improvements in terms of transmit power control for previously selected active transmitter antennas on selected subcarriers. The scheduler algorithm outputs transmit power values for each subcarriers and active antennas. Simulation results show that in high SNR (Signal-to-Noise Ratio) range about 10% gain can be achieved in channel capacity by extending the power control to antennas. Furthermore adaptive *M*-QAM modulation per subcarrier for Rayleigh-fading channel model was introduced allowing better prediction of realistic channel capacity.

Along this paper a brief summary of OFDM and OFDMA downlink transmission is presented, a draft of the so called water-filling (or water-pouring) transmit power allocation algorithm and its complexity is shown. The MIMO radio access technique is examined regarding the overall system capacity and its optimization tasks in Section 3. The MIMO-OFDMA system model is proposed for locating partial tasks in transmission architecture. A reference MIMO-OFDMA RRM (Radio Resource Management) solution is introduced in Section 4, which allocates radio resources in case of MIMO-OFDMA transmission, providing proportional fairness among users. Practical improvements on the reference algorithm described above are presented in Section 5, where adaptive power control for antennas is discussed in details in Section 6. Section 7 deals with simulation results followed by the conclusion in Section 8.

## 2. Multiple antenna transmission

The multi-antenna transmission- and receptions schemes have the name MIMO in the related literature. MIMO schemes can be characterized into three main groups: beam forming solutions, frequency- and space-diversity schemes and *spatial multiplexing* (SM). Spatial multiplexing is often referred as MIMO in itself. In this paper we will be consider spatial multiplexing exclusively.

### 2.1 Spatial multiplexing

During the spatial multiplexing mode, different data symbols are transmitted on the radio link by different antennas on the *same frequency and time interval*. Multipath propagation is assumed for the efficient operation of spatial multiplexing, i.e. rich multipath scattering increases the capacity of the MIMO channel, and LOS (line of sight) propagation degrades strongly the performance of MIMO [8]. The MIMO transmission can be characterized with a time-variant channel matrix according to (2.1)

$$\mathbf{H}(\tau,t)=\begin{pmatrix} h_{1,1}(\tau,t) & h_{1,2}(\tau,t) & \cdots & h_{1,N_{\mathrm{R}}}(\tau,t) \\ h_{2,1}(\tau,t) & \ddots & & \\ \vdots & & h_{n_{\mathrm{T}},n_{\mathrm{R}}}(\tau,t) & \vdots \\ & & & \ddots \\ h_{N_{\mathrm{T}},1}(\tau,t) & \cdots & & h_{N_{\mathrm{T}},N_{\mathrm{R}}}(\tau,t) \end{pmatrix}$$

where $h_{n_{\mathrm{T}},n_{\mathrm{R}}}(\tau,t)$ represents the complex time-variant channel transfer function at the path between the $n_{\mathrm{T}}$-th transmitter antenna and the receiver antenna $n_{\mathrm{R}}$. $N_{\mathrm{T}}$ and $N_{\mathrm{R}}$ represent the number of transmitter and receiver antennas respectively.

#### 2.1.1 Capacity of MIMO channel

Derived from Shannon's law, the following expression was proven in [8] and [9] for the capacity of a MIMO channel

$$C=\max_{tr(\mathbf{R_{ss}})\le p}\log_2(\det(\mathbf{I}+\mathbf{H}\mathbf{R}_{ss}\mathbf{H}^{\mathrm{H}})), \qquad (2.2)$$

where **H** denotes the channel matrix defined in (2.1), $\mathbf{H}^{\mathrm{H}}$ denotes the transpose conjugate of **H**, **I** represents an identity matrix with a flexible size, and let denote $\mathbf{R}_{ss}$ the covariance matrix of the transmitted signal vector **s**. However, (2.2) has a considerably uncomfortable form for practical applications. Hereinafter, we will investigate the transformation of the MIMO channel into parallel SISO (Single Input, Single Output) channels in order to apply a similar expression to calculate the equivalent capacity like Shannon's formula.

#### 2.1.2 Capacity of parallel equivalent SISO channels

As it is shown in [10], if singular value decomposition (SVD) [11] is applied to MIMO channel matrix, expression (2.2) can be transformed into a more convenient form, which is equivalent to calculate the aggregate Shannon-like transmission rate (in bit/s) of multiple independent SISO channels.

$$C=B\cdot\sum_{i=1}^{M}\log_2\left(1+\frac{\varepsilon_i^2\cdot p_i}{N_0}\right). \qquad (2.3)$$

In the expression above $B$ and $N_0$ represent the channel bandwidth and the spectral power density of the additive white Gaussian noise (AWGN) respectively. $\varepsilon_i$ denotes the $i$-th singular value of the **H** channel matrix, where $i\in\{1,2,...,M\}$. The $\varepsilon_i^2$ values are equivalent to the eigenvalues of the matrix $\mathbf{H}\cdot\mathbf{H}^{\mathrm{H}}$, often referred in literature as $\lambda_i(=\varepsilon_i^2)$. $M=\min(N_{\mathrm{T}},N_{\mathrm{R}})$ denotes the number of independent SISO channels and $p_i$ represents the transmit power allocated on the $i$-th equivalent SISO channel. The (real) values of $\varepsilon_i^2$ contain both the effects of the average *channel gain*, and the *spatial correlation* of the channel paths within the MIMO constellation. Note, if the MIMO channel paths are independent, and the capacity will be maximal, and $\varepsilon_i^2=\varepsilon_j^2$, for $\forall i\neq j$.

*Figure 1. MIMO-OFDMA System Model*

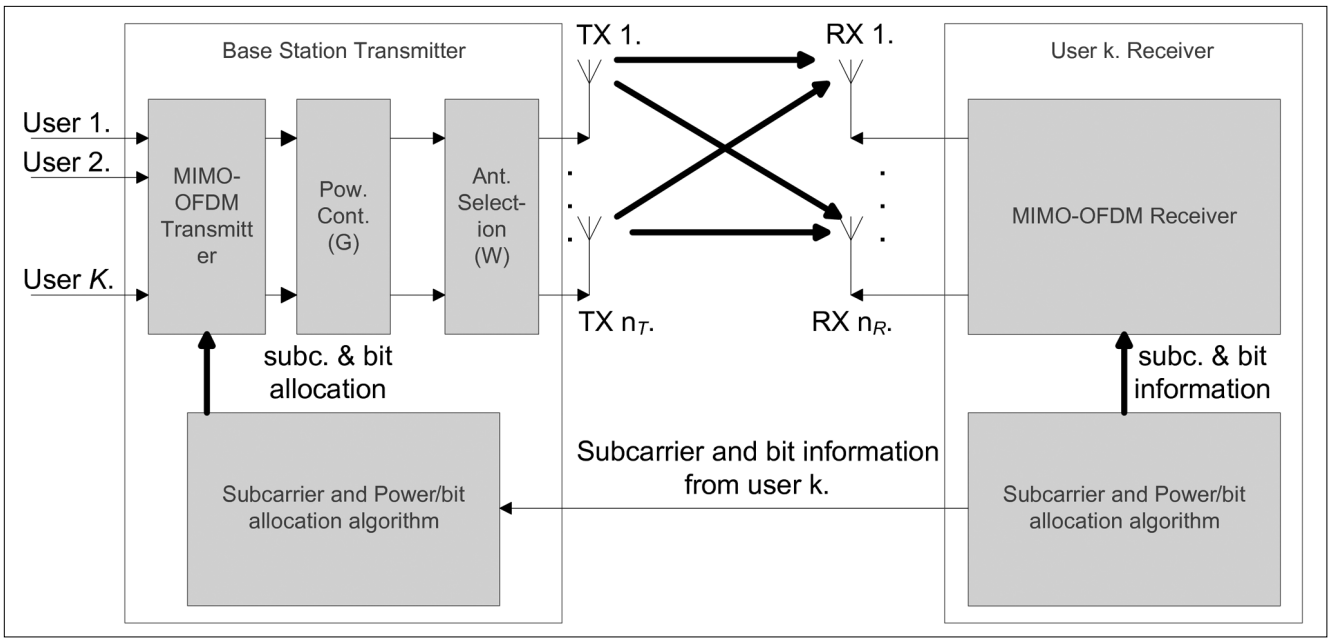

## 3. MIMO-OFDMA system model

In this section, a model will be provided for MIMO-OFDM radio transmission, a MIMO-OFDM block scheme and the optimization potentials will be summarized.

### 3.1 MIMO-OFDMA

A system model of downlink MIMO transmission combined with OFDMA multiple access is illustrated at *Fig. 1.* A subcarrier- and power allocation algorithm is performed at the transmitter side (assuming the availability of CSI information). Each of the transmitter and receiver antennas are assigned to *individual* OFDM transmitters and receivers.

#### *3.1.1 MIMO-OFDMA channel model*

For the characterization of a multiuser MIMO radio channel, some transformations should be performed on a channel model given in section 2.1. Since the radio channel has a frequency selective feature along the subcarriers, and different users have channel paths with different conditions toward the base station, the MIMO channel – defined in (2.1) – needs to be *distinguished* along each $N$ carriers and $K$ users. Completed with the assumption, that the radio channel will be considered constant in time and frequency within the scheduling time intervals, and along the bandwidth of the different subcarriers.

Expression (3.1) describes the the channel matrix – according to (2.1) – for subcarrier $n$, and user $k$.

$$\mathbf{H}_{k,n}=\begin{pmatrix} H_{1,1}^{(k,n)} & H_{1,2}^{(k,n)} & \cdots & H_{1,N_{\mathrm{R}}}^{(k,n)} \\ H_{2,1}^{(k,n)} & \ddots & & \\ \vdots & & H_{n_{\mathrm{T}},n_{\mathrm{R}}}^{(k,n)} & \vdots \\ & & & \ddots \\ H_{N_{\mathrm{T}},1}^{(k,n)} & \cdots & & H_{N_{\mathrm{T}},N_{\mathrm{R}}}^{(k,n)} \end{pmatrix}, \quad (3.1)$$

where $n_{\mathrm{T}}\in\{1,2,...,N_{\mathrm{T}}\}$ and $n_{\mathrm{R}}\in\{1,2,...,N_{\mathrm{R}}\}$ are the indexes of transmitter and receiver antennas, and $H_{N_{\mathrm{T}},N_{\mathrm{R}}}^{(k,n)}$ denotes the complex channel samples according to the *scheduling period* for the different antenna-paths.

During a MIMO-OFDMA transmission it can be easily shown, that for characterization of the *overall* radio channel, the introduction of a 4-dimensional $\mathbf{H}_{\mathrm{tot}}$ hypermatrix is needed with the size of $K\times N\times N_{\mathrm{T}}\times N_{\mathrm{R}}$, according to

$$\mathbf{H}_{\mathrm{tot}}=\begin{pmatrix} \mathbf{H}_{1,1} & \mathbf{H}_{1,2} & \cdots & \mathbf{H}_{1,N} \\ \mathbf{H}_{2,1} & \ddots & & \mathbf{H}_{1,N} \\ \vdots & & \mathbf{H}_{k,n} & \vdots \\ & & & \ddots \\ \mathbf{H}_{K,1} & \cdots & & \mathbf{H}_{K,N} \end{pmatrix}, \quad (3.2)$$

where $\mathbf{H}_{k,n}$ elements are arisen from (3.1).

### 3.2 MIMO-OFDMA system capacity optimization

The capacity optimization task of a MIMO-OFDMA transmission can be generalized as follows (3.3)

$$C=\arg\max_{C,p} B\cdot\sum_{k=1}^{K}\sum_{n=1}^{N}\rho_{k,n}\left[\sum_{i=1}^{M_{k,n}}\log_2\left(1+\frac{\lambda_{k,n}^{(i)}p_n}{N_0}\right)\right],$$

where $\rho_{k,n}$ represents the elements of the $K\times N$ *subcarrier assignment* matrix, where $\rho_{k,n}=1$, if subcarrier $n$ is assigned to user $k$, and $\rho_{k,n}=0$ otherwise. A requirement has to be set for the transmit power allocation:

$\sum_{n=1}^{N} p_n \le P_{max}$, $p_n \ge 0$ for all $k$ and $n$, where $P_{max}$ denotes the maximal transmit power of the MIMO-OFDMA transmitter. The value of $\lambda_{k,n}^{(i)}$ represent the eigenvalue $i$ of $\mathbf{H}_{k,n}\,\mathbf{H}_{k,n}^{\mathrm{H}}$ matrix, where $i=1,...,\mathrm{rank}(\mathbf{H}_{k,n})$.

#### *3.2.1 Subcarrier allocation*

In case of MIMO-OFDMA access, in terms of maximization of the overall system capacity, user $k$ is assigned to subcarrier $n$, for which the following expression will be maximal

$$k_n=\arg\max_{k}\prod_{i=1}^{M_{k,n}}\left(1+\frac{\lambda_{k,n}^{(i)}p_n}{N_0}\right). \quad (3.4)$$

The method above follows the simple OFDMA subcarrier allocation, since subcarrier to be allocated are characterized with a scalar value, however $k_n$ values contain $\lambda_{k,n}^{(i)}$ eigenvalues, which are determined both by the gains of the MIMO path of the MIMO channel indexed by $k$ and $n$, and the degree of linear independence of MIMO paths on the same $k$ and $n$ indexes.

The capacity of OFDMA access can be – in principle – multiplied with a factor, which can be expressed as

$$M_{k,n}=\mathrm{rank}\left(\mathbf{H}_{k,n}\right)\equiv\min\left(N_{\mathrm{T}},N_{\mathrm{R}}\right). \quad (3.5)$$

Note that, in case of MIMO-OFDMA there exist $K\times N$ pieces of channel matrices, and the singular value decomposition and transformation into parallel SISO channel (as seen in 2.1.2) are executed $K\times N$ times.

The practical realization of subcarrier allocation above follows to a computationally complex task. The following two criterions are suggested in [12] to simplify subcarrier allocation, which lead to suboptimal resource allocation

$$k_n^P:=\arg\max_{k}\prod_{i=1}^{M_{k,n}}\lambda_{k,n}^{(i)} \quad (3.6)$$

$$k_n^S:=\arg\max_{k}\sum_{i=1}^{M_{k,n}}\lambda_{k,n}^{(i)} \quad (3.7)$$

called *product-* and *sum* criterions. Product criterion is more efficient in high SNR domains than sum criterion, and vice verse. However, application of MIMO technique is usually relevant by high SNR values, hence product criterion has greater importance in MIMO resource management.

#### *3.2.2 Transmit power control*

A further requirement to maximize the overall system capacity is the allocation of $p_n$ transmit power values for subcarriers, which are the roots of the following equation system

$$\sum_{i=1}^{M_{k,n}}\frac{\lambda_{k_n,n}^{(i)}}{\lambda_{k_n,n}^{(i)}p_n+N_0}+\alpha=0, n\in\{1,2,...,N\}, \quad (3.8)$$

where $k_n$ is the index of user, which owns the carrier $n$, $\alpha$ satisfies the requirement $\sum_{n=1}^{N} p_n = P_{max}$. The method above is referred as the *multi-dimensional water-filling* algorithm, namely for $M_{k,n}$=1. we get the form of 'common' water-filling solution [13].

*3.2.3 Antenna selection*

In MIMO systems the antenna RF (radio frequency) circuits can also be considered as a resource factor during the capacity optimization. The market rates of RF chains do not follow the general rules in computer studies (Moore's law). Thus, by the manufacturing of MIMO radio devices is a main aspect to reduce the number of necessary RF circuits. This consideration gives the reason of existence of so called *antenna selection* algorithms if a MIMO device has multiple transmitter antennas, but there are only $L \leq N_T$ available RF chains. The task of a transmitter side antenna selection algorithm is to select $L$ pieces of antennas, on which the most efficient radio transmission can be realized, based on channel properties on selected chain paths [14].

In optimal case, the expression of the channel capacity is needed to be calculated for $\binom{N}{L}$ cases before each symbol transmission however, this optimal technique can lead to an unacceptable computational complexity likewise. A common algorithm for antenna selection produces near optimal results for transmit side antenna selection with linear operations called Gorokhov's method [15].

## 4. MIMO-OFDMA RRM solution

A reference method [6] will be proposed in this section, which provides a suboptimal solution for the maximization of MIMO-OFDMA capacity expression (3.3) by providing proportional fairness. Subcarrier allocation and power control is realized for selected subcarriers. Listed partial tasks are handled separately to give a treatable computational complexity and thus, suboptimal results. The performance (spectral efficiency) of the algorithm is evaluated by Shannon's formula, giving a loose upper bound for system capacity, which is not feasible for analyzing the performance of the algorithm in a standardized telecommunication network.

### 4.1 Objectives of the reference algorithm

Product criterion – defined in (3.6) – is used for subcarrier allocation purposes. Proportional fairness is ensured among users, which means, that a defined quotient $\{\gamma_k\}_{k=1}^{K} / R_k$ should be equal for each user, where $\{\gamma_k\}_{k=1}^{K}$ represents a vector, containing the transmission rate relations between different users, and $R_k$ denotes the actual transmission rate of user $k$, which can be calculated according to (3.3) with the Shannon's formula.

$$R_k = \sum_{n=1}^{N} \rho_{k,n} \left[ \sum_{i=1}^{M_{k,n}} \log_2 \left( 1 + \frac{\lambda_{k,n}^{(i)} \cdot p_n}{N_0} \right) \right] \qquad (4.1)$$

The partial tasks of the proposed algorithm will be detailed in the following subsections.

### 4.2 Subcarrier pre-allocation

During this phase, the $N_k$ number of allocated subcarriers will be calculated for each user based on $\{\gamma_k\}_{k=1}^{K}$. This pre-allocation step will be executed according to a calculated $\overline{H_k}$ average channel gain values for each user according to

$$\overline{H}_k = \frac{1}{N_T \cdot N_R} \frac{1}{N} \sum_{n=1}^{N} \sum_{n_T=1}^{N_T} \sum_{n_R=1}^{N_R} |H_{k,n}|, \forall k \qquad (4.2)$$

where $H_{k,n}$ is already defined in (3.1). Equal power distribution is assumed on subcarriers in order to reduce complexity, and an approximated average transmission rate can be calculated for each user

$$\overline{R}_k = N_k \log_2 \left( 1 + \frac{\left|\overline{H}\right|^2 \cdot \overline{P}_k}{N_0} \right) \qquad (4.3)$$

An iterative $N_k$ calculation will be executed. In each step $\overline{R_k}$ is updated, and the user with the lowest $\{\gamma_k\}_{k=1}^{K} / R_k$ quotient will obtain a new subcarrier.

### 4.3 Subcarrier assignment

After determining the number of subcarriers for each user, the effective subcarrier assignment will be executed. Users are divided into two groups according to their $\overline{H_k}$ average channel gain values.

$$\overline{H}_1 \leq \overline{H}_2 \leq ... \leq \overline{H}_k \leq ... \leq \overline{H}_K \qquad (4.4)$$

At first, users with low average channel gain have the possibility to choose the 'best' subcarriers characterized with the $k_n$ lambda product values (3.6). This step allows the compensation of low channel gains for a subcarrier which has high lambda product value, since eigenvalues of MIMO paths are carrying the degree of linear dependency of antenna paths as well. Therefore a reliable transmission can be kept up by a relative low channel gain, the degree of the linear dependency among MIMO paths is relatively low. The subcarrier allocation happens as described in section 4.2, refreshing $R_k$ according to expression (4.1), till each user obtains the $N_k$ number of subcarriers calculated beforehand. After allocation of subcarriers, the transmit power allocation will be performed on selected subcarriers based on (3.8).

## 5. Improvements on MIMO-OFDM RRM

In this section, extensions will be proposed to enhance the efficiency of the reference algorithm, in terms of systems' transmission rate and to make the results to be interpretable for a practical telecommunication system (LTE, WiMAX, etc.). Adaptive $M$-QAM modulation is realized on the selected subcarriers, based on the instantaneous channel state information. Antenna selection and power control for selected antennas will be performed over the subcarriers.

### 5.1 Adaptive M-QAM modulation in Rayleigh-fading channel

For analyzing the operation of a MIMO-OFDMA resource management algorithm in a real communication system, a capacity calculation of a specific modulation method is needed. In 3GPP LTE and WiMAX *M*-QAM adaptive modulation is performed on groups of neighboring subcarriers. However – in principle –, there is a possibility to perform adaptive modulation for each subcarrier.

The task of adaptive modulation can be summarized as the definition of signal-to-noise-ratio (SNR) *domains*, in which the performance of the selected modulation method (or level) will be maximal in terms of spectral efficiency. For solving the problem above, we calculate the channel capacity for different *M* levels of QAM modulation based on analytical bit error results on Rayleigh-fading channel.

#### *5.1.1 Error rates of M-QAM in Rayleigh-fading channel*

Analytical bit error probability expression for *M*-QAM modulation in Rayleigh-fading channel is available according to [16] and [17]:

$$P_b = \frac{2}{\pi\sqrt{M}\log_2\sqrt{M}} \sum_{k=1}^{log_2\sqrt{M}} \sum_{i=0}^{\left(1-2^{-k}\right)\sqrt{M}-1} \left\{ (-1)^{\left\lfloor \frac{i2^{k-1}}{\sqrt{M}} \right\rfloor} \times \right.$$

$$\times \left( 2^{k-1} - \left\lfloor \frac{i2^{k-1}}{\sqrt{M}} + \frac{1}{2} \right\rfloor \right) \qquad (5.1)$$

$$\left. \int_0^{\frac{\pi}{2}} \prod_{l=1}^{L} M_{\gamma_l} \left( -\frac{(2i+1)^2 3/(2(M-1))}{\sin^2\theta} d\theta \right) \right\}$$

$$\text{where} \qquad M_{\gamma_l} = \frac{1}{1-s\bar{\gamma}_l} \qquad (5.2)$$

represents the moment generating function (MGF) of *l*-th branch of applied diversity method in case of Rayleigh-fading channel, and

$$M_{\gamma_l} = \frac{1+K}{1+K-s\bar{\gamma}_l} e^{\left[\frac{Ks\bar{\gamma}_l}{(1+K)-s\bar{\gamma}_l}\right]} \qquad (5.3)$$

denotes the MGF for Rician channel.

#### *5.1.2 Channel capacity*

For a given bit error probability, the capacity of the radio channel for a given SNR can be calculated in closed form pursuant to the following steps. We invoke the expression of the conditional entropy according to [18] and [19]. The spectral efficiency of a binary channel (in bit/s/Hz) expressed with the conditional entropy function, can be calculated as

$$C_{\text{M-QAM}} = \log_2 M \left(1 - H\left(X|Y\right)_{M-QAM}\right), \qquad (5.4)$$

where

$$H(X|Y)_{M-QAM} = \\ -\left[(1-P_b)\log_2(1-P_b) + P_b \cdot \log_2(P_b)\right], \qquad (5.5)$$

denotes the conditional entropy function.

#### *5.1.3 Adaptive modulation on subcarriers*

The task of adaptive modulation is the calculation of SNR levels for *switching* between modulation levels. The essential parameter for bit error probability calculation is the SNR.

Let *us* denote it with $\gamma_n$, and expressed for subcarrier *n* as

$$\gamma_n = \frac{|H_n|^2 P_n}{N_{0,n} \cdot \Delta f_c} = \frac{E_{s_n}}{N_{0,n}} = \frac{E_{b_n} \log_2(M_n)}{N_{0,n}} \qquad (5.6)$$

where $P_n$ denotes the allocated transmit power (in W), $E_{s_n}$ and $E_{b_n}$ represent the *received* symbol- and bit energy for subcarrier *n* respectively, $N_{0,n}$, $\Delta f_c$ and $M_n$ nominates the spectral power density of the AWGN, the subcarrier spacing (in Hz) and the modulation level on subcarrier *n*.

After that, the modulation levels can be determined obviously for each SNR (or transmit power) domain. At *Fig. 2*, the capacity curves of QPSK (4-QAM), 16-QAM and 64-QAM are plotted for different $E_{b_n}/N_0$ levels, and the intersections of the curves determine the modulation switching points, to provide the maximal spectral efficiency.

*Figure 2. M-QAM levels for adaptive modulation by different $E_{b_n}/N_0$ levels*

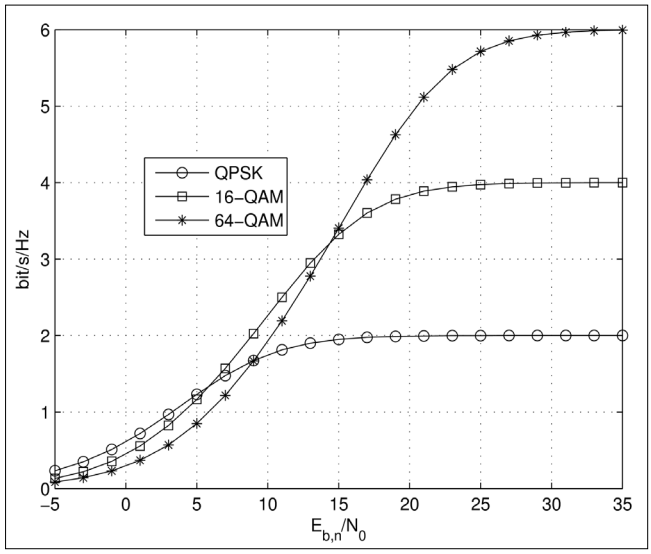


### 5.2 Antenna selection at the transmitter side

As it was exposed in section 3.2.3, $L = \min(N_T, N_R)$ number of transmitter antennas should be assigned to available transmitter RF devices transmission for maximizing capacity, if $N_T \geq N_R$. For realizing computationally efficient antenna selection method, antenna specific channel state information is needed as the input of the algorithm. Similarly to expression (4.2), the average channel gain values can be derived from $\mathbf{H}_{k,n}$ matrices given in (3.1).

At the first step, let define an $N_T \times N_R$ average $\mathbf{H}_{aver}$ channel gain matrix according to

$$\mathbf{H}_{\text{aver}} = \frac{1}{K}\frac{1}{N}\sum_{k=1}^{K}\sum_{n=1}^{N}|\mathbf{H}_{k,n}|\,. \qquad (5.7)$$

A further transformation will be accomplished on $\mathbf{H}_{aver}$ to obtain $N_T$ pieces of scalar values, characterizing transmitter antennas. $\mathbf{H}_{aver}$ will be transformed into a $\mathbf{h}_{n_T}$ vector with

$$\mathbf{h}_{n_T} = \frac{1}{N_R}\sum_{n_R=1}^{N_R}\mathbf{H}_{\text{aver}}, \qquad (5.8)$$

with that, the antenna selection algorithm selects the first $L$ largest elements from $\mathbf{h}_{n_T}$ in each scheduling interval

$$\arg\max_{n_T} \frac{1}{N_R} \sum_{n_R=1}^{N_R} h_{n_T,n_R}, \tag{5.9}$$

realizing statistical antenna processing gain in terms of spectral efficiency compared to the random selection of transmitter antennas. (See simulation results in Section 7.)

## 6. Adaptive power control for antennas

The reference method – presented in Section 4 – stops at the power control for subcarriers, and assumes equal power distribution along the transmitter antennas. However, the allocated power values for subcarriers can be divided further, based on the eigenvalues of $\mathbf{H}_{k,n}$ matrices. Since the rank of $\mathbf{H}_{k,n}$ equals with the number of selected $N_T$ antennas, eigenvalues can be ordered to the corresponding transmit antennas. The power control task could be naturally contracted, however in order to hold the optimization task in computational complexity, it is practical to separate the two power control tasks after all. In this case, the elements of a $\beta_n^{(i)}$ vector shall be calculated during the following formalized task according to Shannon's formula (6.1)

$$\arg \max_{\beta \in \mathbb{R}^{N \times M_{k,n}}} \sum_{k=1}^{K} \sum_{n=1}^{N} \rho_{k,n} \left[ \sum_{i=1}^{M_{k,n}} \log_2 \left( 1 + \frac{\lambda_{k,n}^{(i)} \beta_n^{(i)} p_n}{N_0} \right) \right],$$

so that $\sum_{i=1}^{M_{k,n}} \beta_n^{(i)} = 1, \forall n \qquad \leq \beta_n^{(i)} \leq 1$ while $\forall i, n.$ values are independent over the carriers, the optimization problem can be separated into $N$ pieces of maximization tasks. It is noticeable, that the optimization task defined in expression (6.1) is very similar to the general water-filling problem with the modification, that subcarriers' channel gain vector is transformed into SISO $\lambda_{k,n}^{(i)}$ eigenvalues, and the number of subcarriers will be represented by $M_{k,n}$. At *Fig. 3*, the capacity of a 3 antenna scenario is illustrated along different $\beta_n^{(i)}$ power distributions. The reason of existence of antenna power allocation can be well observed, because the maximum of capacity is not located at $\beta_n^{(1)}=\beta_n^{(2)}=\beta_n^{(3)}=1/3$.

*Figure 3. Capacity function of 3-antenna system by different power allocation*

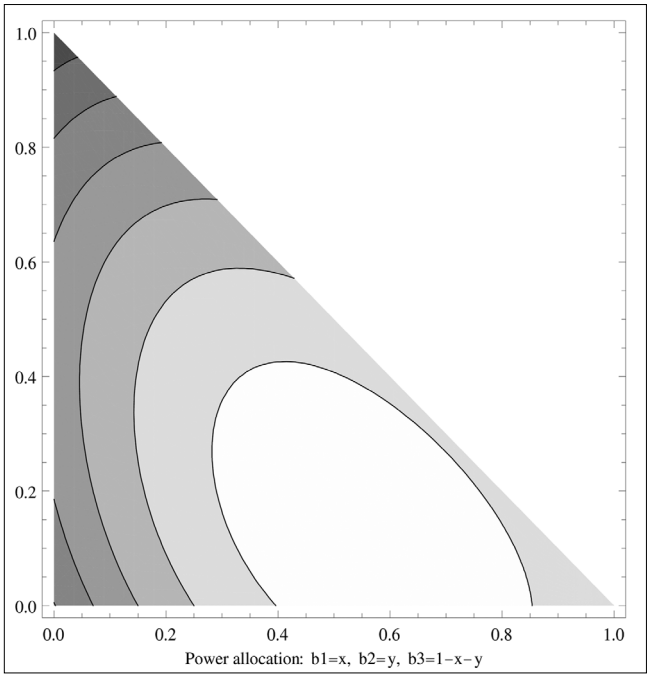


The water-filling solution is available, and is formalized in Equation (3.8). After the appropriate transformations mentioned above, the antenna power allocation algorithm can be formalized as follows

$$\beta_n^{(i)} + \frac{N_0}{\lambda_{k,n}^{(i)} \cdot p_n} - \alpha = 0, i = 1, 2, ..., M_{k,n}. \tag{6.2}$$

The defined method has the advantage, that the computation can be parallelized, resulting significant acceleration in calculation. Let note, that maximizing Shannon's capacity does not provide the optimal solution in a communication system, which operates with real $M$-QAM modulation. Realization of so-called bit loading water-filling [13] exceeds the confines of this paper.

| Parameter | Notation | Value |
|---|---|---|
| Subcarrier spacing | $\Delta f_c$ | 15 kHz |
| System bandwidth | $W_{OFDM}$ | 5 MHz |
| Number of subcarriers | $N = \lfloor W_{OFDM}/\Delta f_c \rfloor$ | 333 |
| FFT size | $N_{FFT}$ | 512 |
| Sampling frequency | $f_s = N_{FFT} \cdot \Delta f_c$ | 7.86 MHz |
| Symbol period | $T_s = 1/\Delta f_c$ | 66.7 $\mu$s |
| Carrier frequency | $f_c$ | 2.5 GHz |
| AWGN spectral density | $N_0$ | -174 dBm/Hz |
| Cell radius | | 500 m |
| Base station height | | 30 m |
| Mobile station height | | 1.5 m |
| Pathloss model | | COST-HATA-231 |
| LTE signaling overhead | | 27.29 % |

*Table 1. Simulation parameters*

## 7. Simulation results

The performance results, and plots are mainly based on analytical calculations (Shannon's capacity and $M$-QAM capacity), however some of the system parameters – like user's position within cells, complex Rayleigh-fading channel coefficients, and users' fairness vector – were randomly generated.

### 7.1 System Parameters

For analyzing performance of scheduler algorithm LTE radio access, parameters were considered in *Table 1*.

### 7.2 Illustration of operation

*Fig. 4* illustrates a scheduling cycle in case of $K=6$ users. Channel gain parameters are randomly generated (first row). For the sake of simple illustration, fairness parameters are set to $\gamma=(1,1,1,1,1,5)$. The allocated carriers to users can be observed at the third row, to provide

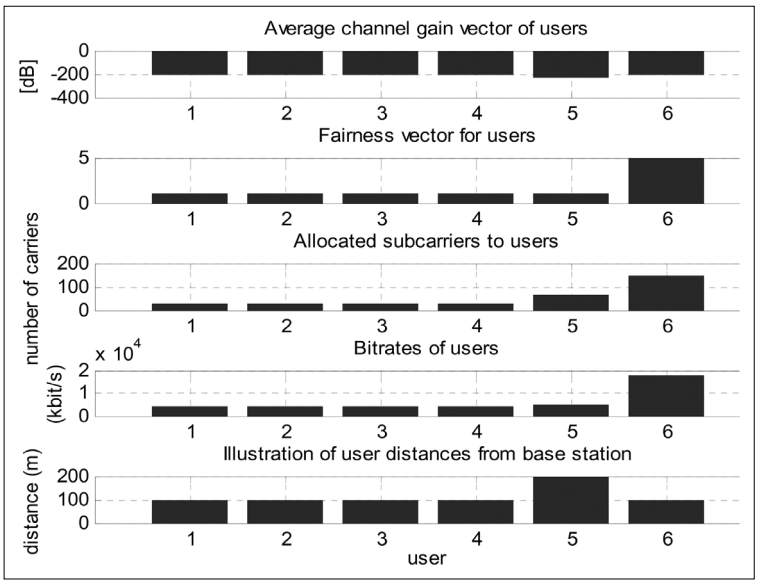


*Figure 4. Illustration of a scheduling cycle*

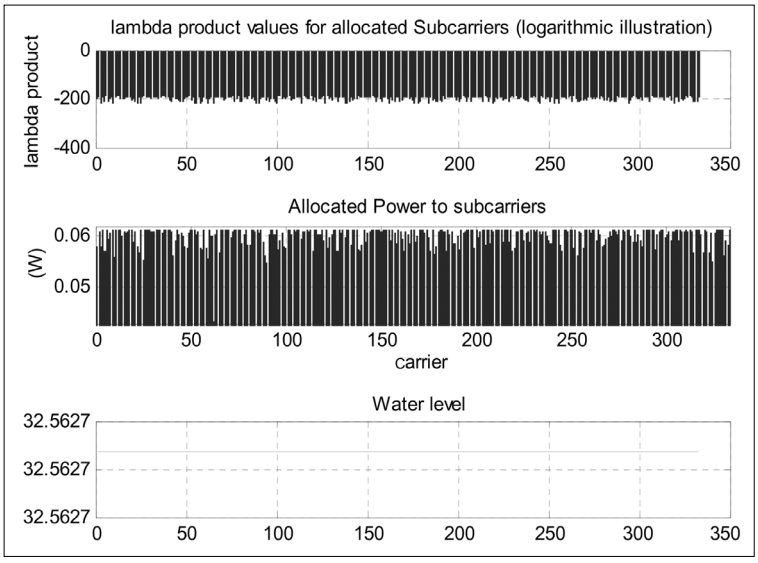


*Figure 5. Adaptive Transmit Power Control over subcarriers*

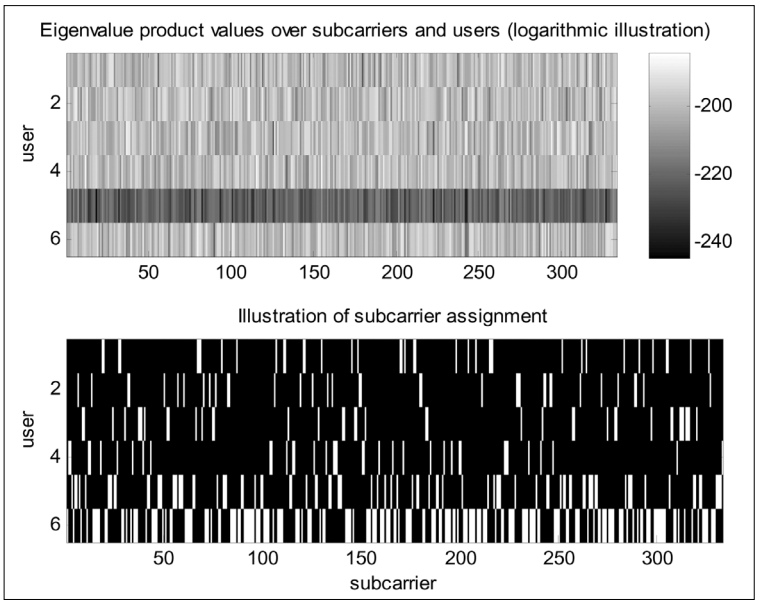


*Figure 6. Illustration of MIMO-OFDMA singular value products, and subcarrier assignment*

achievable transmission for users. The fulfillment of fairness requirements is visible, even if channel gain distribution has a large deviation for certain subcarriers.

The results of the multi-dimensional water-filling (defined in section 3.2.2) are illustrated on *Fig. 5*. The proper operation of the algorithm can be checked with equal $\alpha$ 'water level' for each subcarrier.

The results of the subcarrier allocation – based on lambda product values – are depicted at *Fig. 6*. At the upper diagram, the lambda product values are shown for each subcarrier and user (in logarithmic scale). User 5 (which has the largest distance from base station) has the minimal average $\prod_{i=1}^{M_{k,n}} \lambda_{k,n}^{(i)}$ value (row 5). Lower part of Fig. 6 contains the illustration of the subcarrier allotment. It seems that user 6 (which has the largest proportional fairness parameter) has obtained the main part of subcarriers. In addition, user 5 (which has equal fairness parameter with first 4 users) have received more carriers than first 4 users to balance the penalty resulting from its lower average channel gain values.

### 7.3 Performance analysis

In the following steps, the performance analysis will be summarized of the reference method completed with new elements, discussed in Section 5. We have illustrated the spectral efficiency as a function of the $E_s/N_0$ quotient at the transmitter-side. The set-up and the *randomly generated* channel coefficients implied a path attenuation of approximately 100 dB, which the transmitted signal was exposed to in our simulations.

#### *7.3.1 User distances and System capacity*

In Section 4.1, the overall system capacity and fairness were presented as contradictory aspects. At *Fig. 7*, at first equal (100 m) user distance were set as an input of the scheduling, resulting 81.82 Mbit/s of overall system transmission rate. However, this situation can be considered fairly infrequent in real conditions. On the right side of the figure, the first user's location were set to 400 m from the base station.

In this case (maintaining fairness) the scheduler has allocated almost all of the subcarriers for that user, resulting significant degradation in overall (76.61 Mbit/s) transmission rate.

#### *7.3.2 Fairness analysis*

The widely used Jain's index [20] means a feasible method for analyzing the degree of fairness. Jain's index provides a value between 0 and 1.

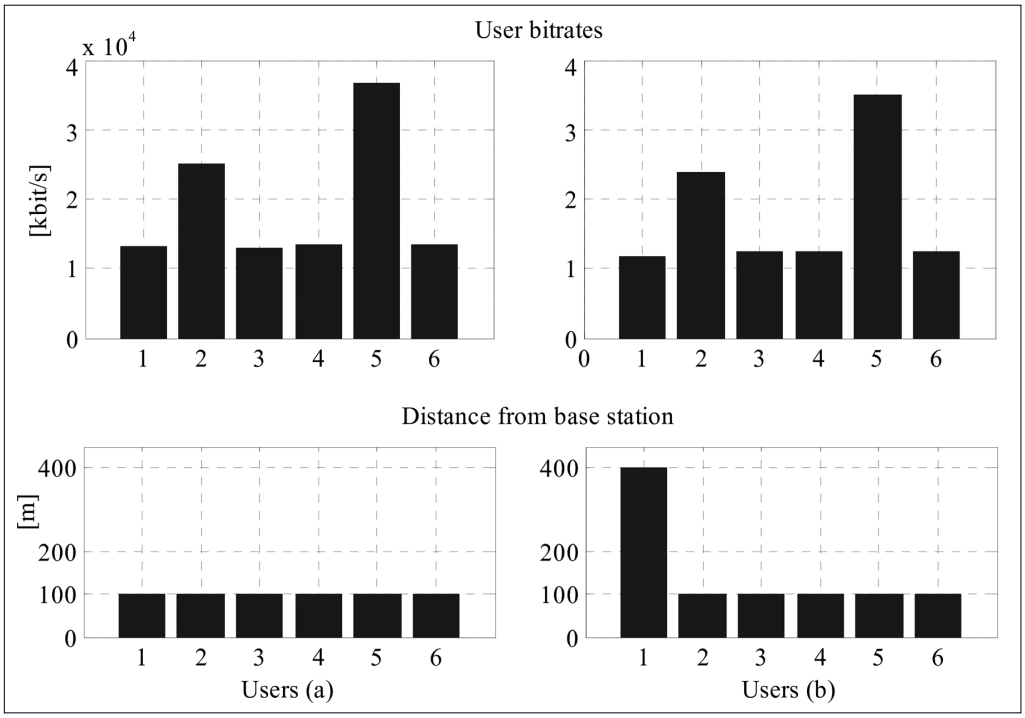


*Figure 7. Effect of user distances on system capacity*

$$f(\bar{r}) = \frac{\left(\sum_{k=1}^{K} \frac{R_k}{\phi_k}\right)^2}{K \sum_{k=1}^{K} \left(\frac{R_k}{\phi_k}\right)^2}, \qquad (7.1)$$

where $\phi_k$ could be an amount of money, which user $k$ pays for the service, proportional to its desired transmission rate. At *Fig. 8*, the Jain's fairness index is illustrated by growing number of users.

Curves were calculated by fixed distances, but different channel coefficients. It can be observed, that growing antenna number produces decreased fairness, even by extended system bandwidth (20 MHz) and transmit power (20 W). A reason for lower fairness values by growing antenna numbers can be that the effect of the distances has a greater influence on lambda products.

### *7.3.3 MIMO performance*

*Fig. 9* illustrates the spectral efficiency of MIMO by different transmit power levels and antenna arrangements. In literature of MIMO technology a common statement holds, that performance of MIMO transmission grows with SNR, and application of MIMO is worthy by high SNR values. Two kind of propagation environments (rural and urban) are simulated in terms of propagation loss (differences between two environments in terms of complicated scattering environment is not modeled). In terms of propagation loss, rural (dotted lines) environment provides better SNR results. The lower part of Fig. 9 illustrates the fraction of 4x4 MIMO and SISO channel for the rural case. The curve of the rural environment is located on the top for all transmit power values. This can be explained only with lower propagation loss (higher SNR) in rural environment.

In a real scattering environment this effect should be turned over, because the degree of scattering significantly affects the capacity of a MIMO channel. However, exact modeling of different MIMO environments could be the subject of a distinct work.

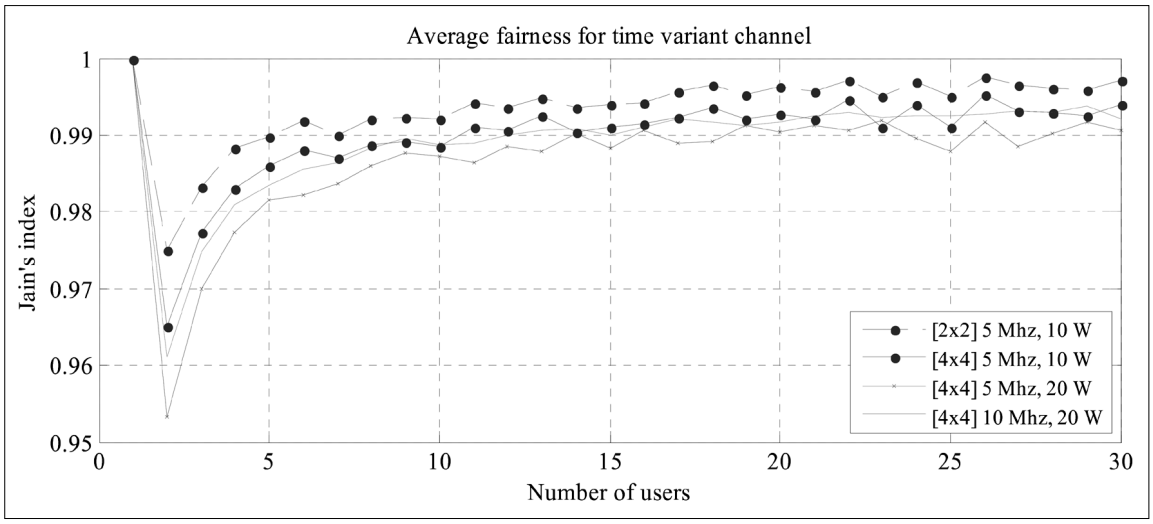


*Figure 8. Illustration of fairness by different MIMO scenarios*

*7.3.4 Adaptive modulation*

*Fig. 10* shows the spectral efficiency of different MIMO antenna scenarios calculated from Shannon's capacity, and adaptive *M*-QAM capacities. The application of *M*-QAM modulation does not provide any spectral efficiency gain of course, however it can illustrate the performance of the MIMO transmission (and scheduling algorithm) in a realistic transmission system with adaptive *M*-QAM modulation. During the simulation, 50 cycles were averaged for alternating MIMO channel coefficients. Transmit power was divided equally among subcarriers and antennas.

*7.3.5 Power Control*

*Fig. 11* contains the results of spectral efficiency of power control, calculated by Shannon's formula. Three cases have been distinguished for each antenna configurations: equal power distribution for subcarriers and antennas (continual and dashed lines with no marking), adaptive power control only on subcarriers (cont. and dashed lines marked with 'x'), and adaptive power control for subcarriers and antennas alike (cont. and dashed lines marked with diamonds). On the left side, two MIMO configurations are illustrated in lower transmit power domain, at the right side both configurations seem in higher domains. In higher SNR domains full (both over carriers and antennas) power allocation curve accommodates to the curve of the equal power distribution, and it's visible that power control provides a 10-12% gain at lower SNR values.

At *Fig. 12*, the same simulation is illustrated with the difference, that spectral efficiency has been calculated according to the capacity expression of *M*-QAM given in Section 5.1. The 'full' power allocation method provides spectral efficiency gain at low SNR values likewise, while in high SNR domains the performance of power control will turn over. In a practical realization adaptive power control should be turned out in high SNR domains.

## 8. Conclusion

As an improvement of the referenced MIMO-OFDMA RRM solution defined in Section 4, a new downlink resource allocation algorithm was developed, which maximizes the overall spectral efficiency of the system with certain constraints.

The constraints were selected with respect to practical applications: proportional fairness is a suitable representation of QoS the mobile stations can be provided with. The proposed algorithm results in power allotment over subcarriers which allows the base station to meet the requirements, while the overall system capacity is kept closer to the optimum, than it was in the proposed reference work. Planning phases were interpreted, which separate the complex (NP-hard) optimization problem into distinct – independently executable – subtasks (i.e subcarrier allocation, adaptive modulation, antenna selection, transmit power control over subcarriers and antennas). Interpreted separation results the manageability of the proposed optimization problem. Nevertheless, the execution of separated optimization tasks is only able to result suboptimal radio resource management. The current work is not supposed to quantitati-

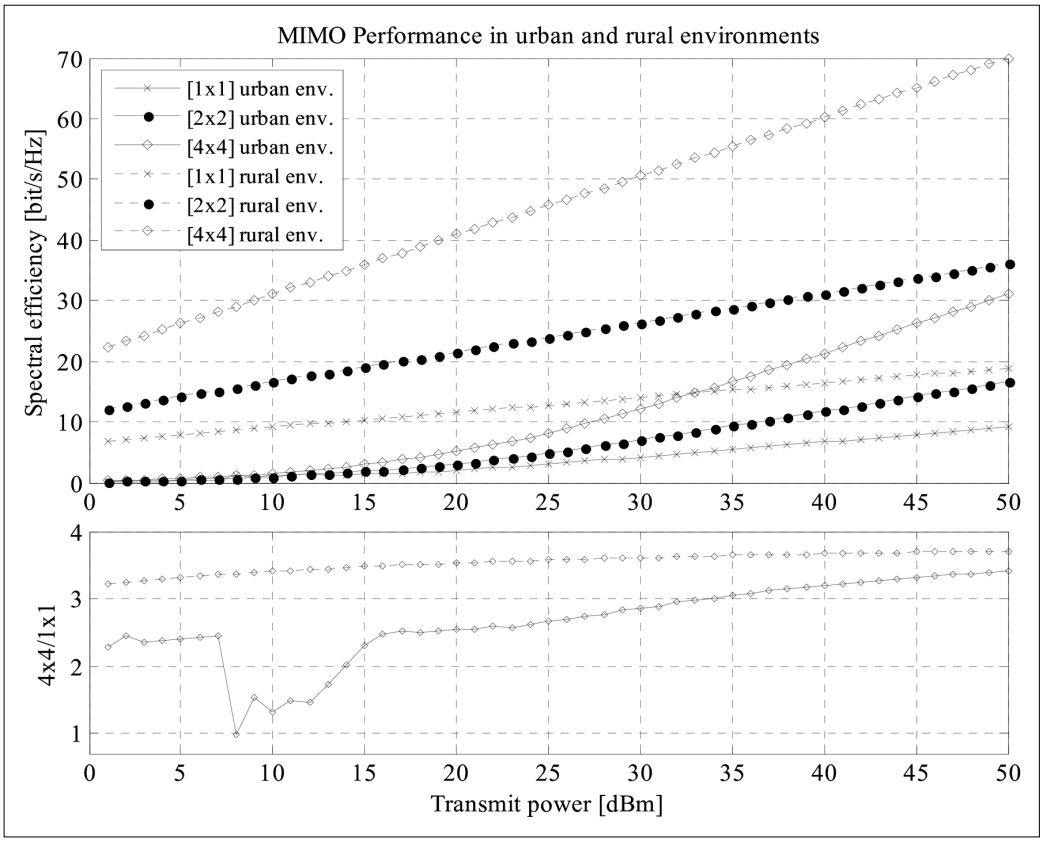


*Figure 9. MIMO performance by different propagations environment*

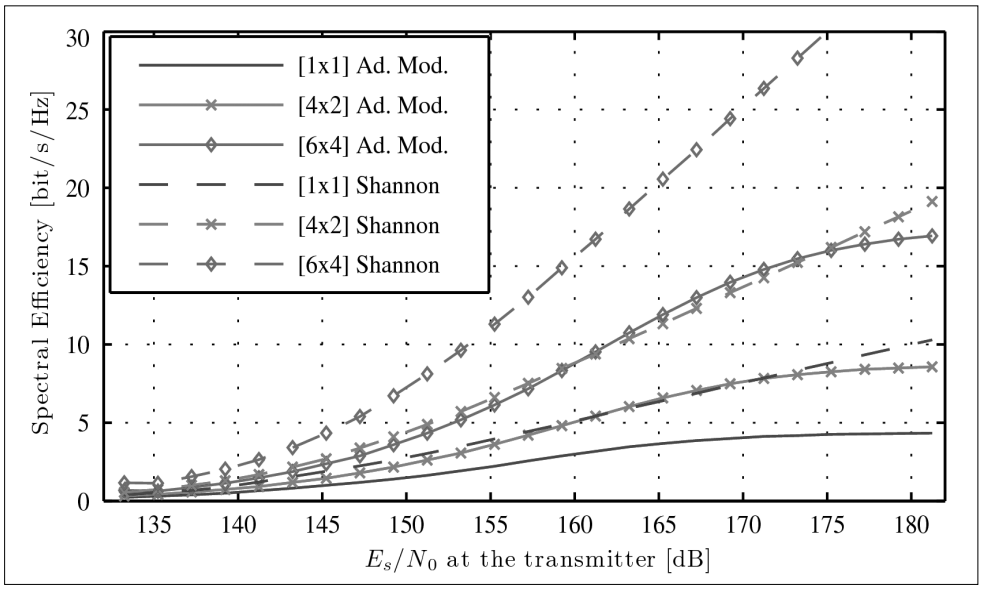


*Figure 10. M-QAM adaptive modulation's capacity compared to theoretical capacity*

vely analyze the measure of how far the resulted power distribution is from the optimum solution. However we can declare a couple of things qualitatively.

Splitting the set of users up into two groups along the users' measured channel parameters is a fairly rough approach, but this step significantly cuts down on complexity. A refined division of still acceptable complexity could take closer to the optimum. Our proposed amendment however did not lower the complexity either, in comparison with the reference method the additional power allocation step requires more computational capacity at each base station.

Introducing antenna selection causes further divergence from optimum, however efficient selection of an-

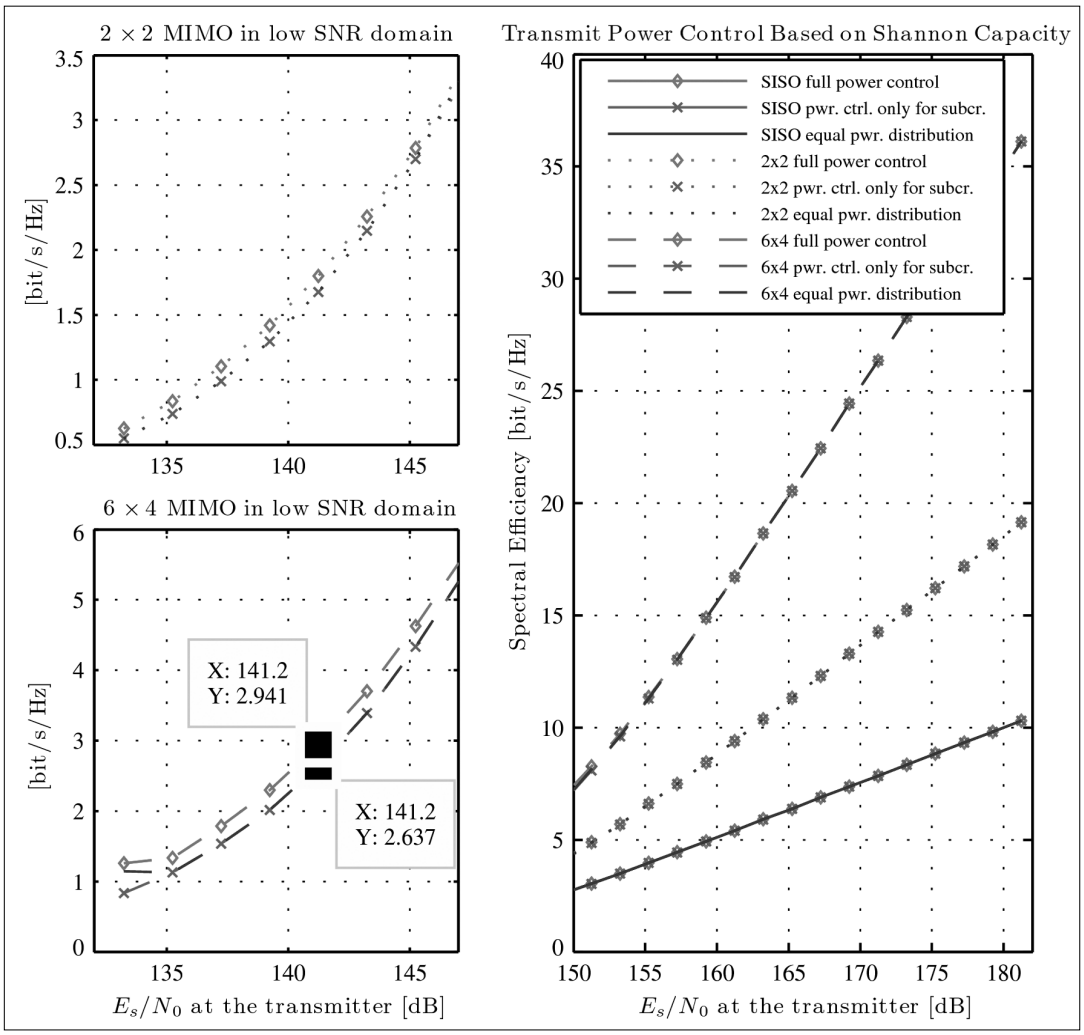


*Figure 11. Shannon capacity of MIMO power control*

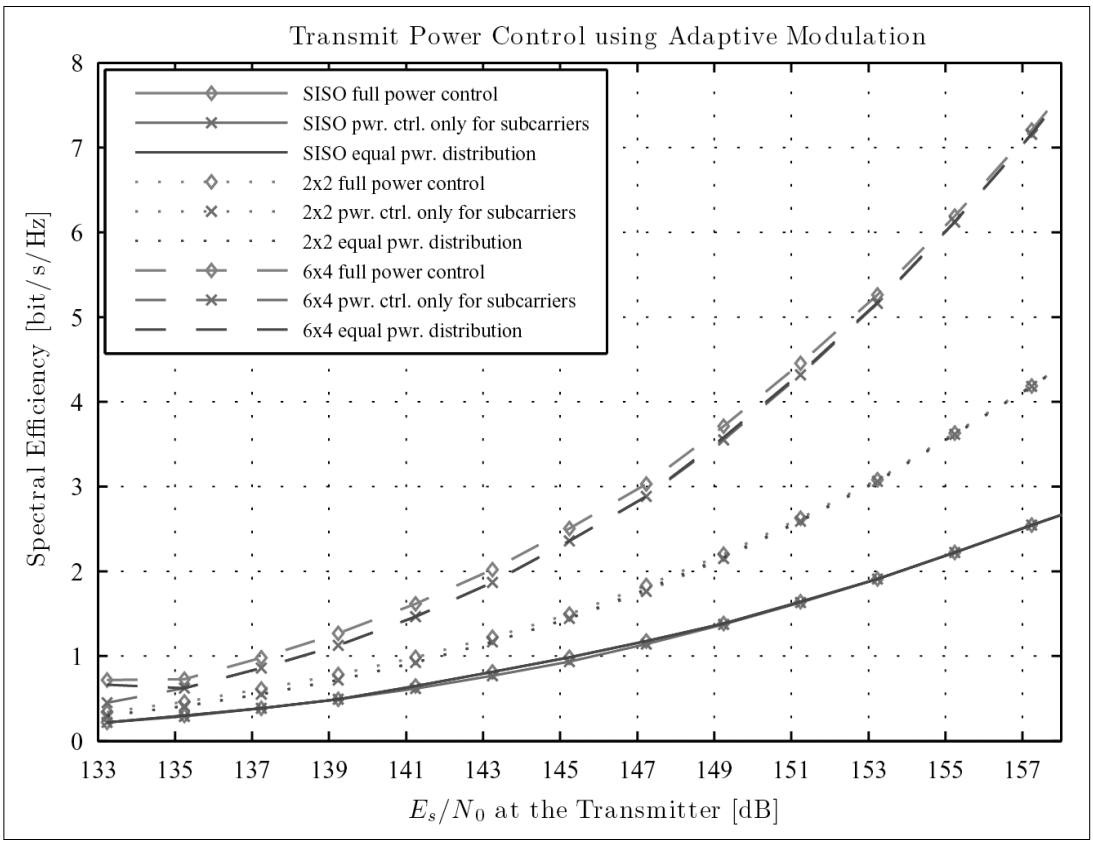


*Figure 12. M-QAM capacity of MIMO power control*

tennas to be cut off could enable significant savings on RF circuits and power demand. A field of improvement of the current work is to evaluate algorithms to be used for antenna selection.

In return for more computational cost with the proposed power control scheme over transmitter antennas the per user transmit rate can be increased by about 10%. Since considerable benefits come forward in the lower SNR region, end user satisfaction can be levered in such situations where the channel properties are less favorable e.g. far away from the base station or in rarely covered area.

The antenna selection and antenna power control mean additive components to the reference RRM algorithm. In addition, the performance evaluation of the proposed algorithm happens assuming adaptive *M*-QAM modulation over the subcarriers, which enables better convergence to Shannon-capacity in multiple SNR domains, than in a case of applying single *M* level of QAM modulation, as well as adaptive modulation allows a more realistic performance evaluation in a standardized communications system. Those simulation results showed which capacity level can be most likely achieved in practical applications.

Of course the performance and thus the actual channel capacity is hardly dependent on the accuracy of Channel State Information fed back to the transmitter. We did not consider channel estimation and equalization methods – inevitable in practical applications – in order to get more realistic results, which is a possible direction to head for.

## Authors


**ALBERT MRÁZ** was born in 1979 in Budapest, Hungary. He received the MSc degree in electrical engineering from the Budapest University of Technology and Economics (BUTE) in 2005. He is currently working toward the PhD. degree at BUTE. His research interests include the modeling and resource management of broadband wireless networks (3G and 4G).

**TAMÁS ZÁMBÓ** received the M.Sc. degree in Computer Science from Budapest University of Technology and Economics (BME) in 2009. He has been taking part in researches at BME Department of Telecommunications. His main field of research interest is 4G mobile telecommunications. At the moment he is employed at Ericsson Hungary as Tool Expert.

**SÁNDOR IMRE** was born in Budapest in 1969. He received the M.Sc. degree in Electrical Engineering from the Budapest University of Technology (BUTE) in 1993. Next he started his Ph.D. studies at BUTE and obtained Dr.Univ. degree in 1996, Ph.D. degree in 1999 and DSc degree in 2007. Currently he is carrying his activities as a Professor and a Head of Department of Telecommunications at BUTE. He is a member of Telecommunication Systems Committee of the Hungarian Academy of Sciences. He participates in the Editorial Board of two journals: Infocommunications Journal and Hungarian Telecommunications. He was invited to join the Mobile Innovation Centre as R&D director in 2005. His research interests includes mobile and wireless systems. His main research interests and contributions are in the areas of various wireless access technologies, mobility protocols and reconfigurable systems.

**References**


[1] D. Tse,
"Optimal power allocation over parallel gaussian broadcast channels,"
Proc. of International Symposium on Information, p.27, 1997.

[2] H. L. Guoqing Li,
"On the optimality of the OFDMA network,"
IEEE Communications Letters,
No. ISSN 1089-7798., pp.438–440, 2005.

[3] I.M.T. IEEE Computer Society and T. Society,
"IEEE standard for local and metropolitan area networks,"
IEEE Std 802.16, Part 16: Air Interface for Fixed and Mobile Broadband Wireless Access Systems,
February 2005.

[4] J. S. Erik Dahlman, Stefan Parkvall and P. Beming,
3G Evolution, HSPA and LTE for Mobile Broadband.
Academic Press, 2007.

[5] I. S. Maung Sann Maw,
"Resource allocation scheme in MIMO-OFDMA system for user's different data throughput requirements,"
IEICE Transactions on Communications,
Vol. E91-B, No. 2, 2008.

[6] W. P. Jian Xu, Jongkyung Kim and J.-S. Seo,
"Adaptive resource allocation algorithm with fairness for MIMO-OFDMA system,"
In VTC Spring, No. 63, pp.1585–1589, 2006.

[7] H. Yin and H. Liu,
"An efficient multiuser loading algorithm for OFDM-based broadband wireless systems,"
IEEE Globecom, Vol. 1, pp.103–107, August 2000.

[8] A. van Zelst,
"MIMO-OFDM for wireless LAN,"
Ph.D. dissertation,
Eindhoven University of Technology, April 2004.

[9] J. G. D.S. Shiu, J. Foschini and J. Kahn,
"Fading correlation and its effect on the capacity of multielement antenna system,"
IEEE Transactions on Communications,
Vol. 48, p.502, 2000.

[10] G. Tsoulos,
MIMO System Technology and Wireless Communications.
CRC Press, ch. Theory and Practice of MIMO Wireless Communication Systems, pp.32–34, 2006.

[11] E. Telatar,
"Capacity of multi-antenna gaussian channels,"
European Transactions on Telecommunications,
Vol. 10, No. 6, pp.585–596, 1999.

[12] G. L. H. Liu,
"On the optimality of OFDM in multiuser multicarrier MIMO systems,"
In Proc. VTC-2005-Fall Vehicular Technology Conf.,
No. ISSN 1090-3038, pp.2107–2111, 2005.

[13] J. Bingham,
"Multicarrier modulation for data transmission: An idea whose time has come,"
IEEE Communications Magazine,
pp.5–14, May 1990.

[14] M. Z. W. A. F. Molisch,
"Mimo systems with antenna selection,"
IEEE Microwave Magazine,
Vol. 5, No. 1, pp.46–56, March 2004.

[15] A. Gorokhov,
"Antenna selection algorithms for MEA transmission systems,"
In IEEE International Conference on Acoustics, Speech, and Signal Processing, ICASSP, Ed.,
Vol. 3. IEEE, pp.2857–2860, 2002.

[16] Y. D. Cho K.,
"On the general ber expression of one- and two-dimensional amplitude modulations,"
IEEE Transacions on Communications,
Vol. 50, No. 7, pp.1074–1080, July 2002.

[17] M. Simon and M. Alouini,
Digital communication over fading channels: a unified approach to performance analysis.
John Wiley and Sons, 2002.

[18] T. M. K. Granino A. Korn,
Mathematical Handbook for Scientists and Engineers: Definitions, Theorems, and Formulas for Reference and Review.
Dover Publications Inc., March 2003.

[19] C. Arndt,
Information Measures: Information and its Description in Science and Engineering.
No. ISBN 3-540-41633-1, ch. Channel Information, pp.370–373, Berlin, Springer, 2001,

[20] K. Fall,
"EECS instructional and electronics support,"
Online lecture.